

Application of Effective Stress Intensity Factors to Crack Growth Rate Description

A. F. Liu*

Northrop Corporation, Hawthorne, California

An extensive review on fatigue crack growth rate descriptions has been conducted. An effective stress intensity expression $\Delta K_e (= U \cdot \Delta K)$, with $U = U_0 + (1 - U_0)\beta^{(1-R)}$ has been developed. This expression for U contains only two empirical constants and is derived based on the concept of crack closure. Its capability to account for the R -ratio effect on crack growth rate has been demonstrated by making correlations with experimental data sets containing data points of both positive and negative R ratios. An existing effective stress intensity expression, i.e., Walker's $\overline{\Delta K} (= \Delta K/(1-R)^{1-m})$, has also been examined. A procedure for fitting a sigmoidal curve through the normalized data points (having ΔK_e or $\overline{\Delta K}$ as an independent variable) is presented.

Introduction

THE ability to describe accurately constant amplitude crack growth rate behavior is an essential element in today's computerized methodology for spectrum cracks growth life prediction. The magnitude of this problem can be appreciated by examining some typical experimental data, such as those shown in Figs. 1 and 2.^{1,2} It is seen that the crack growth rate, i.e., the amount of crack increment per stress cycle (da/dN) is a function of stress intensity range (ΔK) and R (defined as the ratio of minimum to maximum cyclic stress). It is customary to fit a curve through all the data points of a given R and then use an equation to represent the fitted curve. Each da/dN curve can be divided into three regions, i.e., a slow-growing (so-called threshold) region, a linear region (the middle section of the curve), and a terminal region (toward the end of the curve at high ΔK values). Although some of the R ratios (in these figures) do not include a clearly defined threshold or terminal region, the existence of these regions has been well recognized.³⁻⁸ Therefore, a crack growth rate equation should both represent a curve of sigmoidal (S) shape and fit the data for all the R ratios.

Over the past twenty years, many crack growth rate equations have been published in the literature. Among these, some dealt with normalizing the R -ratio effect,⁹⁻¹⁴ the mathematical formulation of a sigmoidal curve,¹⁵⁻¹⁹ or both.^{20,21} Some divided the equation into multiple segments attempting to obtain a closer fit between experimental data and an equation.^{22,23} For those equations containing an effective stress intensity parameter, the parameter is often inadequate for normalizing the R -ratio effect over a wide range of R ratios. For example, the Forman equation fails to show correlation between crack growth rates and negative R . Also, the Walker equation requires two effective ΔK parameters, one for positive R and another for negative R . Sigmoidal equations, or equations containing multiple empirical coefficients, require separate sets of empirical constants for each R ratio.

The primary objective of the present investigation is to develop a single crack growth rate equation that can use a single set of empirical constants to fit all the data. This objective has been accomplished by taking the following approaches:

- 1) Develop an effective stress intensity expression that can normalize crack growth rate data (da/dN vs absolute ΔK) over a range of positive and negative R ratios.
- 2) Develop a general formula that can fit a sigmoidal curve through all the normalized experimental data points.

The secondary objective of the present investigation is to investigate the possibility of using an existing effective stress intensity expression to reach the same goal of the primary objective. It is shown that this objective can be accomplished by combining the Walker equation and the sigmoidal equation developed in step 2 above.

Background on Crack Growth Rate Equations and Methods for Handling the R -Ratio Effect

Since Paris^{24,25} published the first crack growth rate equation based on fracture mechanics, no less than 30 such equations have been suggested. The original Paris power law correlated fatigue crack growth rate under constant amplitude loading with the stress intensity range as

$$\frac{da}{dN} = C \cdot \Delta K^n \quad (1)$$

where C and n are material constants. The relationship between the crack growth rate da/dN and the stress intensity range ΔK is a straight line on a log-log plot, and C and n are the intercept and slope of the line, respectively. The power law described the crack growth behavior well for a given R (the minimum-to-maximum stress ratio) and the medium range of ΔK (i.e., the linear region of the da/dN data).

The physical significance of the slow-growth and the terminal regions is that there are two obvious limits of ΔK in a da/dN curve. There is a lower limit, the threshold value ΔK_0 , implying that cracks will not grow if $\Delta K < \Delta K_0$, i.e., $da/dN \rightarrow 0$ if $\Delta K - \Delta K_0 \rightarrow 0$. On the other hand, if ΔK becomes too large, a static failure will follow immediately, which implies that K_{max} exceeded the fracture toughness K_C , which is equivalent to ΔK exceeding $(1-R)K_C$, i.e., $da/dN \rightarrow \infty$ if $(1-R)K_C - \Delta K \rightarrow 0$. In analytical relations, these limiting conditions can be satisfied by having $\Delta K - \Delta K_0$ in the numerator and $(1-R)K_C - \Delta K$ in the denominator,

Presented as Paper 84-0884 at the AIAA/ASME/ASCE/AHS 25th Structures Structural Dynamics and Materials Conference, Palm Springs, CA, May 14-16, 1984; received June 6, 1984; revision received Dec. 5, 1985. Copyright © American Institute of Aeronautics and Astronautics, Inc., 1985. All rights reserved.

*Senior Technical Specialist, Aircraft Division. Associate Fellow AIAA.

i.e.,

$$\frac{da}{dN} = C \Delta K^n \frac{\Delta K - \Delta K_0}{(1-R)K_C - \Delta K} \quad (2)$$

This equation gives a sigmoidal relation on a log-log plot with two vertical asymptotes. Note that the Forman equation⁸ is actually a partial of Eq. (2), without the $(\Delta K - \Delta K_0)$ in the numerator, i.e.,

$$\frac{da}{dN} = \frac{C \Delta K^n}{(1-R)K_C - \Delta K} \quad (3)$$

The equation handles the linear and upper parts of a da/dN curve.

Although the stress ratio R appears in the denominator of the right-hand side of the above equations, it is not intended to account for the R effect on da/dN ; it only serves to control the upper end of the da/dN curve, i.e.; when K_{\max} approaches K_C , da/dN approaches infinity. This type of formulation actually recognizes the effect of the R ratio on K_C , because the term $(1-R)K_C$ is essentially an effective K_C for a different R ratio, but ignores the real effect of R on crack growth rate behavior.

A common technique for fitting the da/dN data points to a sigmoidal curve has been to select a mathematical function that will display a curve of the sigmoidal shape and then build a crack growth rate equation around it. The da/dN equations of Ref. 15 (based on the inverse hyperbolic tangent function) and Ref. 19 (based on the hyperbolic sine function)

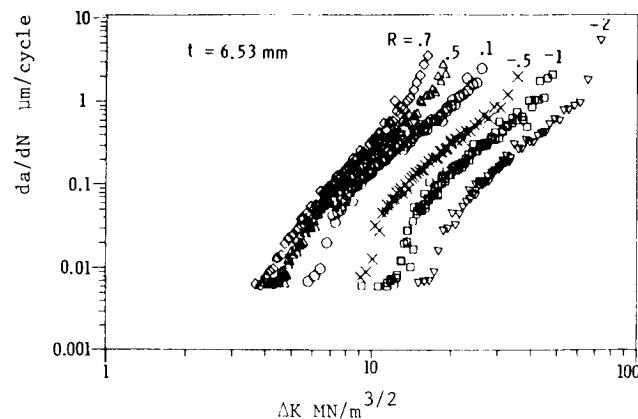


Fig. 1 Experimental crack growth rate data for 2024-T351 aluminum (Ref. 1).

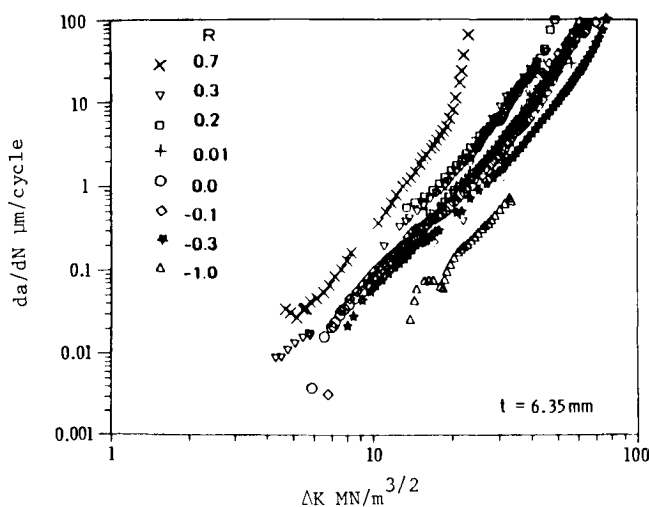


Fig. 2 Experimental crack growth rate data for 2219-T851 aluminum (Ref. 2).

are typical examples. However, these equations can only fit the da/dN data individually, i.e., separate sets of empirical constants are required for each R ratio.

A method to account for the R -ratio effect is to employ a normalizing function on ΔK , i.e., to come up with a common, effective ΔK parameter so that all the da/dN curves (for each individual R) will collapse into one single curve. For example, the Walker effective ΔK parameter was expressed as

$$\overline{\Delta K} = S_{\max}^{1-m} \Delta S^m \sqrt{\pi a} \Phi_i \quad (4)$$

where m is an empirical constant, S the applied stress; a an appropriate crack length, and Φ_i the geometry correction factor on K . This relation eventually reduces to

$$\overline{\Delta K} = \Delta K / (1-R)^{1-m} \quad (5)$$

Figures 3 and 4 are the actual examples showing the collapsed da/dN data points (reduced from the data set of Fig. 1). It is seen that the Walker $\overline{\Delta K}$ requires two m values, one for positive R and another for negative R .

The Walker $\overline{\Delta K}$ parameter is usually used along with the Paris equation, i.e.,

$$da/dN = C \overline{\Delta K}^n \quad (6)$$

and is called the Walker equation. Actually the Walker $\overline{\Delta K}$ can be incorporated into any other existing da/dN equation to handle the R -ratio effect. Jaske et al.²⁰ have used it along with the Colliopriest equation. This combined equation was subsequently used by Swift.²⁶

An alternate method of handling the R -ratio effect is to adjust the C term instead of the ΔK term. This approach has been employed by Saxena and Hudak²² in the three-component model.

The three-component equation,

$$\frac{1}{(da/dN)} = \frac{A_1}{\Delta K^{n_1}} + A_2 \left\{ \frac{1}{\Delta K^{n_2}} - \frac{1}{[(1-R)K_C]^{n_2}} \right\} \quad (7)$$

serves to connect three segments of a da/dN curve into one. The first term on the right-hand side of the equation corresponds to the slow-growth region (without a threshold). The second and third terms correspond to the linear and terminal regions, respectively. It has been claimed that the slopes n_1 and n_2 are independent of R ratios but the intercepts A_1 and A_2 are dependent on R . By determining the coefficients of the intercepts for each R individually and connecting them by means of a linear equation, a da/dN data set (containing several R) can be fitted collectively for all stress ratios. Since there are no fixed functional forms

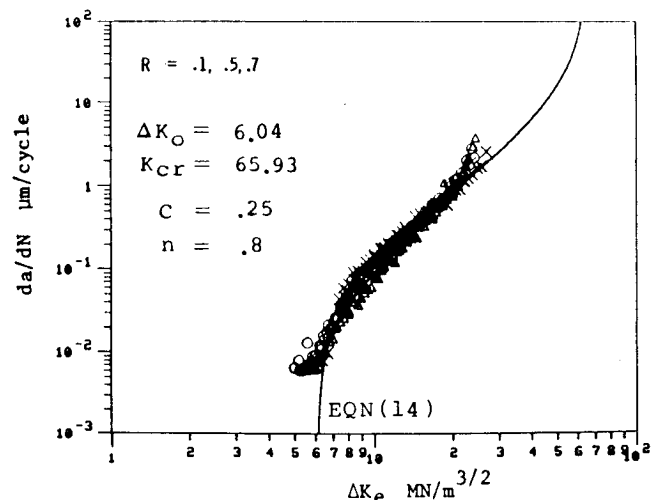


Fig. 3 Normalized 2024-T351 data points; part 1: Walker's $m=0.65$ for positive R ratios.

relating A_1 and A_2 to R it is therefore recognized that this may not be the best method to account for the R -ratio effect.

Development of an Effective Stress Intensity Expression Based on Crack Closure

Following an extensive survey of existing approaches published in the literature, it was apparent that the crack closure-based fitting function approach used by Schijve¹³ and deKoning¹⁴ would be an effective means for developing an effective stress intensity factor as a function of an R ratio. The concept of crack closure considers that material at the crack tip is plastically deformed during fatigue crack propagation. During unloading of a stress cycle, some contact between the crack surfaces will occur due to the constraint of surrounding elastic material. The crack surfaces then remain closed for some time during the following up-loading cycle. It has been further hypothesized that the crack is unable to propagate while it remains closed. This is based on the assumption that the net effect of closure is to reduce the apparent ΔK value to some effective value $\Delta K_e (= K_{\max} - K_{\text{op}})$ i.e., raising the minimum stress intensity factor to the level required to reopen the crack, defined as K_{op} .

Elber²⁷ defined the effective stress intensity range as

$$\Delta K_e = U \Delta K \quad (8)$$

where

$$U = \frac{K_{\max} - K_{\text{op}}}{K_{\max} - K_{\min}} \quad (9)$$

He also showed that U was a function of R . Numerous investigations have since sought to develop experimental techniques to measure crack opening loads for a variety of materials or to investigate the physical mechanism of crack closure. Inconsistencies in measured K_{op} values have frequently been reported in the literature. References 4, 28, and 29 pointed out that K_{op} is dependent on material thickness, R ratio, K_{\max} level, crack length, environment (including frequency and temperature), and, above all, experimental procedure and the definition of crack opening load in a test. In a test coupon, K_{op} changes from the surfaces toward the midthickness of the specimen. The value of K_{op} is also dependent on the smoothness or flatness of the crack faces often associated with small crack sizes or low stress intensity levels, as well as the formation of shear lips at larger crack lengths. Therefore, it would be impossible (and impractical) to try to develop a normalizing function (for ΔK_e) that correlates engineering crack growth rate data from experimental crack closure data. The challenge to an analyst is to select an analytical function for U (as a function of R) and then pair it with a sigmoidal crack growth rate equation to obtain correlations with reasonable degrees of accuracy and consistency. Following is a discussion of the criteria for setting up such an analytical function.

Examining Eqs. (8) and (9), it is clear that for a given R ratio the value of U should be between 0 and 1, i.e., $0 < U \leq 1$. Physically speaking, $U=1$ implies that the crack is fully opened (i.e., $K_{\text{op}}=K_{\min}$) whereas $U=0$ would mean that the crack is fully closed (i.e., $K_{\text{op}}=K_{\max}$). Setting U greater than 1 implies that K_{op} is below K_{\min} , i.e., the crack will open before the upraising local reaches K_{\min} . At the present time it is believed that this is physically impossible (if there is such a case, it will be outside the scope of this paper). Since numerous experimental data indicate that U is an increasing function of R , it is conceivable that U may reach an asymptotic limit $U_0 (>0)$ when R approaches $-\infty$. For a given stress cycle, one may define

$$R_e = K_{\text{op}}/K_{\max} \quad (10)$$

where $K_{\text{op}} \geq K_{\min}$. Since $R = K_{\min}/K_{\max}$, therefore $R_e \geq R$, and R_e can be a negative value as long as it is greater than, or equal to, its corresponding value for R . In addition, the finite element analysis results of Newman³⁰ have shown that R_e should decrease as R decreases.

Since both Eqs. (9) and (10) contain a K_{op} term, there is a unique relationship between U and R_e . Dividing both the denominator and the numerator of Eq. (9) by K_{\max} , one may obtain

$$U = (1 - R_e)/(1 - R) \quad (11)$$

Therefore any analytical function selected for U should satisfy all the criteria set for both U and R_e , i.e.,

$$U_0 \leq U \leq 1$$

with

$$U_0 > 0$$

and

$$R \leq R_e < 1 \quad (12)$$

The following is an analytical function for U that satisfies the criteria of Eqs. (12), i.e.,

$$U = U_0 + (1 - U_0)\beta^{(1-R)} \quad (13)$$

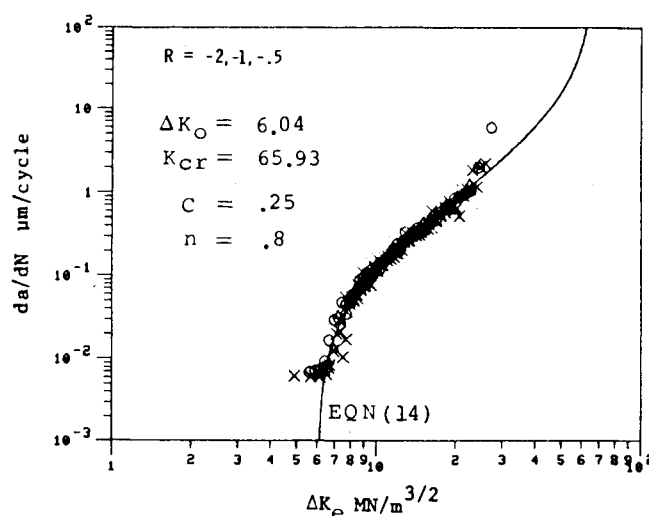


Fig. 4 Normalized 2024-T351 data points; part 2: Walker's $m=0.10$ for negative R ratios.

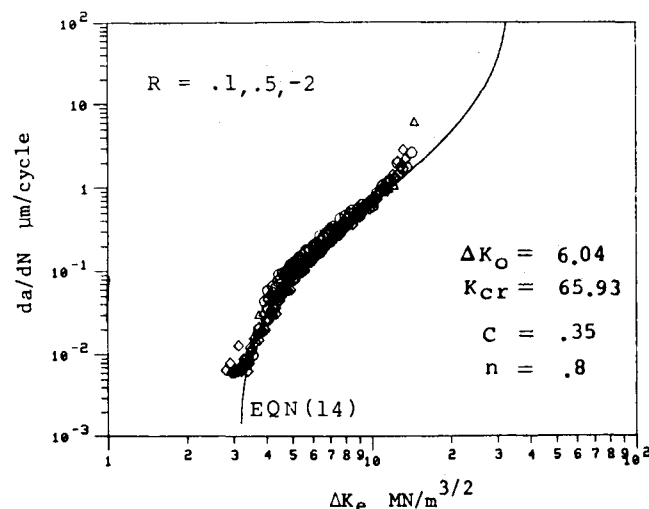


Fig. 5 Comparison of Eq. (14) and normalized 2024-T351 data points (with $\beta=0.45$ and $U_0=0.12$), part 1.

where β and U_0 are empirical constants (depending on material, thickness, and environment) with U_0 being the asymptotic limit for R approaching $-\infty$.

By trial and error, a pair of β and U_0 values could be determined for a given data set. It was found that the 2024-T351 data set (shown in Fig. 1) could be normalized by using $\beta=0.45$ and $U_0=0.12$, and the 2219-T851 data set (shown in Fig. 2) could be normalized by using $\beta=0.5$ and $U_0=0.12$. For purposes of clarity, the normalized data points for the 2024-T351 aluminum were arbitrarily divided into two groups (randomly mixed positive and negative R) and presented in Figs. 5 and 6. The results for the 2219-T851 aluminum are presented in Fig. 7. Again, for clarity, only three R ratios (-1 , 0 , and 0.7) are shown in Fig. 7.

Plotting a Sigmoidal Curve

To plot a sigmoidal curve through a normalized (da/dN vs ΔK_e) data set, simply use Eq. (2), except that all the stress intensity parameters in that equation would have to have effective values, i.e., Eq. (2) becomes

$$\frac{da}{dN} = C \Delta K_e^n \frac{\Delta K_e - \overline{\Delta K}_0}{\overline{K}_{cr} - \Delta K_e} \quad (14)$$

Here $\overline{\Delta K}_0$ and \overline{K}_{cr} are, respectively, the effective value of ΔK_0 , and K_{cr} ; ΔK_0 is the threshold value of stress intensity range at $R=0$; K_{cr} is the critical stress intensity factor for unstable fracture, which we can treat as the upper limit of stress intensity range for $R=0$. The parameters C , n , $\overline{\Delta K}_0$, and \overline{K}_{cr} are the four basic empirical constants needed to display a da/dN vs ΔK_e curve sigmoidally on a log-log scale plot. From Eqs. (8) and (13), we have

$$\Delta K_e = \Delta K [U_0 + (1 - U_0)\beta^{(1-R)}] \quad (15)$$

and

$$\begin{aligned} \overline{\Delta K}_0 &= \Delta K_0 \cdot \overline{U} \\ \overline{K}_{cr} &= K_{cr} \cdot \overline{U} \end{aligned} \quad (16)$$

where

$$\overline{U} = U_0 + (1 - U_0)\beta \quad (17)$$

is a special case of U , for $R=0$.

As mentioned earlier, a crack growth rate equation only defines the shape of a curve; any useful effective K parameter can be placed in Eq. (14) to plot a normalized

curve of a sigmoidal shape. In the case of Walker's $\overline{\Delta K}$, the ΔK_e , the ΔK_0 , and K_{cr} in Eq. (14) will be

$$\begin{aligned} \Delta K_e &= \Delta K / (1 - R)^{1-m} \\ \overline{\Delta K}_0 &= \Delta K_0 \\ \overline{K}_{cr} &= K_{cr} \end{aligned} \quad (18)$$

It is seen that a given set of crack growth rate data points composed of various R ratios can be normalized by using Eqs. (15) or (18). A sigmoidal curve can be fitted through these normalized data points by using Eq. (14), with ΔK_e as an independent variable. Illustrations are given in Figs. 3-7. It should be noted that the curves in Figs. 5 and 6 are two identical curves because they were plotted by using the same empirical constants. These curves were independent of R due to the fact that the original data points had been normalized by U .

As for using the Walker $\overline{\Delta K}$ approach, a sigmoidal curve was drawn through each group of the already compressed da/dN data (see Figs. 3 and 4). Note that the curves in Figs. 3 and 4 are also identical to each other although different m values were used to compress the data because m was not a part of Eq. (14), in which ΔK_e was used as independent variable.

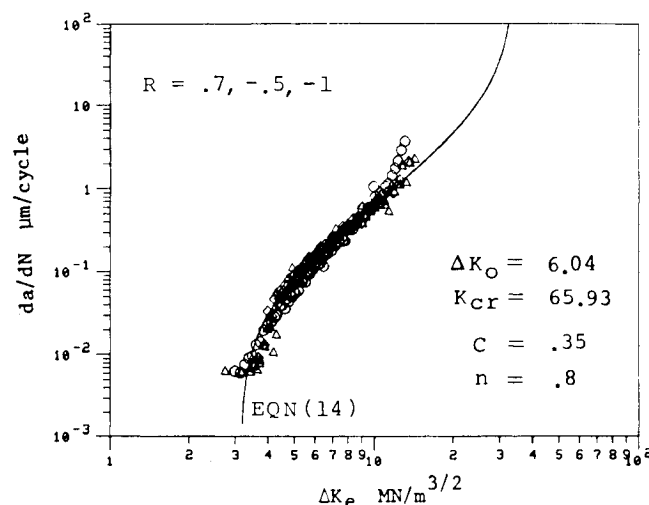


Fig. 6 Comparison of Eq. (14) and normalized 2024-T351 data points (with $\beta=0.45$ and $U_0=0.12$), part 2.

Table 1 Comparison of experimental and analytical lives for 2024-T351 constant amplitude tests at six R -ratios

Specimen no.	R	S_{max} , MPa	a_0 , mm	Experiment		Eqs. (18) & (19) ^a		Eqs. (15), (16) & (19) ^b	
				a_f , mm	N_T , cycles	N_w , cycles	N_w/N_T	N_L , cycles	N_L/N_T
A-2-3	0.7	51.421	22.574	63.055	760670	610000	0.802	630000	0.828
A-2-6	0.7	80.172	14.827	56.864	261980	245000	0.935	265000	1.011
A-2-2	0.5	37.859	20.161	66.103	623280	745000	1.195	595000	0.955
A-2-5	0.5	54.076	13.653	58.452	270570	350000	1.294	300000	1.109
A-2-1	0.1	36.051	14.891	61.925	206360	280000	1.357	310000	1.502
A-2-4	0.1	31.178	18.129	62.579	267540	350000	1.308	380000	1.420
A-2-9	-0.5	31.178	13.875	61.277	298380	375000	1.257	325000	1.089
A-2-10	-0.5	24.098	22.987	53.467	330020	407500	1.235	325000	0.985
A-2-11	-1.0	31.421	14.922	61.373	234560	255000	1.087	230000	0.981
A-2-12	-1.0	24.051	21.653	65.881	373440	420000	1.125	330000	0.884
A-2-13	-2.0	31.302	17.304	62.325	162520	155000	0.954	160000	0.984
A-2-14	-2.0	22.360	21.336	46.228	355130	390000	1.098	355000	1.0
						$\overline{X} =$	1.137		1.062
						$S_x =$	0.171		0.202

^a Empirical constants: $m^{(+)} = .65$, $m^{(-)} = .10$, $C = .25$, $n = .8$, $\eta = 1.0$, $\gamma = 0.5$, and $\lambda = .6$; $\Delta K_0 = 6.04 \text{ MN/m}^{3/2}$, and $K_{cr} = 65.93 \text{ MN/m}^{3/2}$.

^b Empirical constants: $\beta = .45$, $U_0 = .12$, $C = .35$, $n = .8$, $\eta = 1.0$, $\gamma = .05$, $\lambda = .6$; $\Delta K_0 = 6.04 \text{ MN/m}^{3/2}$, and $K_{cr} = 65.93 \text{ MN/m}^{3/2}$.

Examining Figs. 3-7, it is noticed that the normalized data points diverge at the ends. The divergence implies that the normalization function U was only applicable to a portion of the plot, i.e., the linear region. Based on the crack closure point of view, this is not an unexpected phenomenon because crack opening load K_{op} , and U and R_e are functions of applied K levels as well as crack lengths. For the time being we cannot develop a family of U as functions of R and K_{max} , or R and crack length. A temporary solution to this problem has been attained by adding empirical functions to Eq. (14) to control the end points. This approach is justified by considering that ΔK_0 and K_{cr} are also functions of R . Adopting a generalized power function, i.e., $(1-R)$ to the n th power, originally used by Klesnil and Lukas³ to account for the R -ratio effect on ΔK_0 , Eq. (14) has been modified to become

$$\frac{da}{dN} = C \eta \Delta K_e^n \frac{\Delta K_e - \overline{\Delta K_0} \cdot \gamma}{K_{cr} \cdot \lambda - \Delta K_e} \quad (19)$$

where $\overline{\gamma} = (1-R)^\gamma$, $\overline{\lambda} = (1-R)^\lambda$, and $\overline{\eta} = (1-R)^\eta$, of which γ , λ , and η are empirical constants that depend on material, thickness, and environment. The third term η is needed for making a final adjustment because the supplemental terms γ and λ may have overcorrected the linear region of the fitted curve. An improvement is seen by comparing the solid lines [Eq. (19)] and the dotted line [Eq. (14)] in Fig. 7.

Discussion

The present work involves two areas of cyclic crack growth rate description. One area is the implementation of effective stress intensity factors to account for stress ratio effect on crack growth rate. This task can be accomplished by selecting an existing effective stress intensity expression from the literature, e.g., Eq. (18), or by developing a new one, i.e., Eqs. (15-17). Another area deals with fitting a curve through the cyclic crack growth rate data points, i.e., Eqs. (14) and (19). Comments on these approaches are in order.

1) For all practical purposes, the crack closure based effective stress intensity factor approach of this paper may be regarded as the same as those used by Schijve,¹³ deKoning,¹⁴ and Swift²⁶ except that:

a) Both Schijve and deKoning only dealt with the linear region of da/dN . They both developed their effective stress intensity factors based on an anticipated trend in R_e rather than U . The function for R_e was developed first; the func-

tion for U was then obtained through Eq. (11). Hence, the function of U was a quadratic, of which the value of U decreases from $R=1$ to a minimum at $R=-1.75$ and increases again. The fact that U increases in the negative R region and eventually exceeds unity is physically unrealistic. Hence, the applicable range of this U function is very limited ($-1.75 \leq R \leq 1.0$).

b) deKoning used two functions for R_e ; one for positive R (a fourth-power polynomial) and another for a narrow range of negative R (linear between -1.0 and 0). Again the usefulness of this approach is limited.

c) Swift actually picked an existing sigmoidal crack growth rate equation that included Walker's effective ΔK parameter (i.e., the equation of Ref. 20). Once he discovered that the equation did not correlate well with experimental data, he computed the factors (based on the ratio of test life to analytical life) for each R ratio and performed a fifth-power polynomial fit to these factors as a function of R . This polynomial function was then used together with the basic crack growth rate equation. This technique (plotting the test-life-to-analytical-life ratio as a function of R) was quite similar to plotting U as a function of R . Although it (the test-life to analytical-life ratio) could be regarded as a substitute for U , it was, however, obtained from a set of analytical results, and these might vary depending on the initial crack length and possibly a number of other factors. Therefore, this technique may eventually have limited usefulness.

2) The effective stress intensity factor ΔK_e of the present investigation has been developed based on U . The trend of R_e (as a function of R) was used as a supplemental criterion to ensure that the criteria for both U and R_e , i.e., Eq. (12), would be satisfied. Unlike a polynomial for R_e , a cubic for Schijve and a fourth-power function for deKoning, or a fifth-power polynomial for the test-life-to-analytical-life ratio used by Swift, the U function developed in this investigation consists of only two coefficients, β and U_0 . The values of β and U_0 are easily attainable. Since U_0 is an asymptotic limit at $R = -\infty$, it is conceivable that the value of U_0 would be somewhat, but insignificantly, higher than zero. It seems that $0 < U_0 < 0.15$ would be a suitable range for aluminum alloys. On the other hand, based on data published in the literature, the value for U (equivalent to the Elber U for $R=0$) is between 0.4 and 0.6 for aluminum alloys. Since $\beta = (\overline{U} - U_0)/(1 - U_0)$, and $U_0 \approx 0.1$, the value for β is always slightly lower than \overline{U} , i.e., it is possible to estimate the value of β from a narrow range of the anticipated values for \overline{U} .

3) For crack growth analysis it has been a conventional practice to cut off the compression portion of a stress cycle, i.e., assume that $\Delta K = K_{max}$ for all the negative R ratios. This assumption implies that crack opening will not occur until K_{min} of a stress cycle is raised to a stress level above zero. The present investigation considers that K_{op} can take place at any negative stress level as long as K_{max} is positive and the criteria for crack closure, i.e., Eq. (12), are satisfied.

4) It should be noted that a change in crack growth rate behavior (i.e., a discontinuity, or an interruption) can be seen in the 2024-T351 data in Fig. 1 for most of the R ratios. The discontinuity occurred at crack growth rates approximately $5 \times 10^{-3} \mu\text{m}/\text{cycle}$. Limited crack growth rate data on 2024-T3 and 7075-T3 thin alloy sheets³¹ also exhibit such a discontinuity at crack growth rates of approximately $5 \times 10^{-3} \mu\text{m}/\text{cycle}$. It is not certain, at the present time, whether this discontinuity is attributable to testing variables or is an intrinsic mechanical behavior of a given material. Many investigations that have dealt with generating threshold crack growth rate data for various materials (including a limited amount of data on the 2024-T3 and the 2219-T851 alloys) have developed experimental data points in a da/dN range as low as $10^{-4} \mu\text{m}/\text{cycle}$.³⁻⁷ Except for some difficulty in interpreting the 2219-T851 data reported

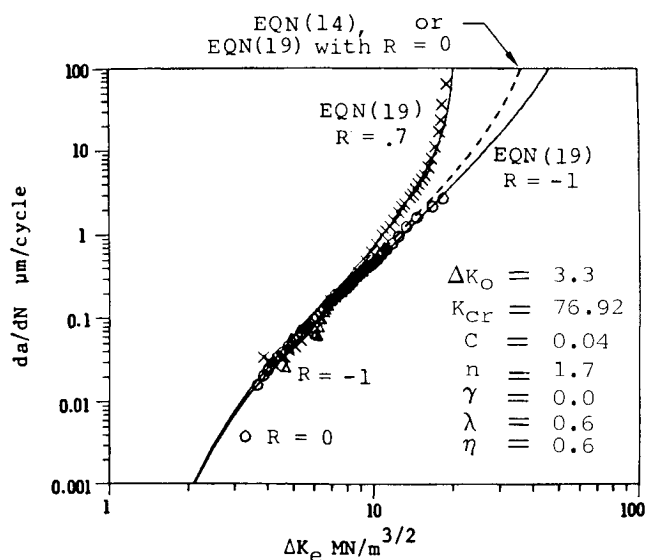


Fig. 7 Comparison of Eqs. (14) and (19) and normalized 2219-T851 data points (with $\beta=0.5$ and $U_0=0.12$).

in Ref. 7, these data generally did not show such a discontinuity. Currently, the American Society for Testing and Materials only publishes standard procedures for generating crack growth rate data at crack growth rates above 10^{-2} $\mu\text{m}/\text{cycle}$. Pending a standardized procedure for generating crack growth rate data below 10^{-2} $\mu\text{m}/\text{cycle}$, there is limited knowledge about the real threshold for each R ratio of a given material, whether a discontinuity should occur, and what to do if a discontinuity indeed exists.

5) To obtain a measure of the accuracy of a chosen crack growth rate description, it is necessary to reconstruct the experimental crack growth histories of a group of tests by using the empirical constants developed for the same set of experimental data. The crack growth lives for the 2024-T351 aluminum specimens have been calculated by using $\Delta\bar{K}$, i.e., Eq. (18), and also U , i.e., Eqs. (15-17), with Eq. (19). As shown in Figs. 3-6, some of the specimens exhibited a discontinuity, i.e., very little change in crack growth rate at stress intensity levels near the $\Delta\bar{K}$ threshold. The sigmoidal curve in each figure was drawn by neglecting those data points at the discontinuity. To make a fair assessment on how accurately these sigmoidal curves can represent the experimental record, each prediction was made by using a selected initial crack length slightly longer than the actual initial crack length of a test; i.e., several data points of the early part of the test had been truncated in order to avoid any problem that would have been caused by the discontinuity. The specifics for each test, i.e., the cyclic stress level (S_{\max}), R ratio, initial and final crack lengths (a_0 , and a_f , respectively), are given in Table 1. The empirical constants used to fit the experimental crack growth data are also listed in Table 1. For each test, the crack growth life, i.e., the number of cycles required for the crack to grow from a_0 to a_f , was calculated. The ratio of the calculated life N_W (based on $\Delta\bar{K}$) or N_L (based on U) to the actual life of the test N_T provides a measure of the accuracy of the methodology. The N_W/N_T and N_L/N_T ratios for each test, along with the mean \bar{X} and standard deviation S_X are given in Table 1. It is shown that by using either method ($\Delta\bar{K}$ or U), the mean for the predicted lives was approximately 10% ($\pm 4\%$) higher than the mean for the experimental lives. It should be noted that the empirical constants used to fit the experimental data were determined by trial and error. They may not represent the best fit for these data sets, but they were used for the purpose of demonstrating how the crack growth rate equations work. No attempt was made to establish actual material allowables.

Conclusions

The present investigation implements a multistep approach to fit experimental da/dN data collectively for all the R ratios. The first step is to treat the data points by using an effective stress intensity factor. It has been shown that both the U factor of this paper and the Walker $\Delta\bar{K}$ are capable of normalizing the R -ratio effect. The issue here is that U has been derived based on the concept of crack closure. It contains only two empirical constants and is a continuous function for a full range of R ratios ($-\infty < R < 1$). The Walker $\Delta\bar{K}$ contains only one empirical constant, but the positive R and the negative R have to be treated separately. The second step is to fit a curve through the already treated data points. In this step, only four empirical constants are required for plotting a sigmoidal curve. It should be mentioned that using ΔK_e (i.e., U or $\Delta\bar{K}$) to normalize the raw da/dN data and fitting a curve through a group of normalized data points are two separate events. These two operations must be performed in sequence. For those data sets that exhibit a change in crack closure behavior at various stages of crack propagation, an expression for U as functions of both R and ΔK will be needed. In this paper, an alternative approach has been implemented. It was handled by incorporating supplemental parameter functions (i.e., $\bar{\gamma}$, λ , and $\bar{\eta}$) into the sigmoidal

equation to adjust the $\Delta\bar{K}_0$ and \bar{K}_{cr} values. It is recognized that studies should be conducted on experimental data containing a large quantity of crack growth rate data points in both the threshold and the terminal regions in order to reconfirm (or update) these empirical relations. The discontinuity behavior observed in the raw da/dN data should be identified by separating the testing variables (if there are any) from material mechanical behavior. Analytical method(s) for handling this problem should be investigated. The applicability of Eqs. (14-19) to other materials such as steels and titanium alloys, and the environmentally assisted crack growth, should also be investigated.

It should be noted that ever since Paris proposed that the stress intensity range (ΔK) was the driving force for fatigue crack propagation, obtaining a reliable description of fatigue crack growth rates has been a common interest of both analysts and experimentalists. Those equations contained in Refs. 8-23 represent only a small sample of the published literature of the past two decades. This paper certainly will not be the last to address this subject. However, it does offer a state-of-the-art approach toward better understanding of the complexity of the problem.

References

- Liu, A. F., "The Effect of Residual Stresses on Crack Growth from a Hole," *AIAA Journal*, Vol. 22, Dec. 1984, pp. 1784-1785.
- Chang, J. B. and Stolpestad, J. H., "Improved Methods for Predicting Spectrum Loading Effects—Phase I Report," AFFDL-TR-79-3606, Vol. II—Test Data, Air Force Flight Dynamics Laboratory, March 1978.
- Klesnil, M. and Lukas, P., "Effect of Stress Cycle Asymmetry on Fatigue Crack Growth," *Materials Science and Engineering*, Vol. 9, 1972, pp. 231-240.
- Sunesh, S. and Ritchie, R. O., "On the Influence of Environment on the Load Ratio Dependence of Fatigue Thresholds in Pressure Vessel Steel," *Engineering Fracture Mechanics*, Vol. 18, 1983, pp. 785-800.
- Schmidt, R. A. and Paris, P. C., "Threshold for Fatigue Crack Propagation and the Effects of Load Ratio and Frequency," *Progress in Fracture Growth and Fracture Toughness Testing*, American Society for Testing and Materials, ASTM STP 536, 1973, pp. 79-94.
- Paris, P. C., Bucci, R. J., Wessel, E. T., Clark, W. G. Jr., and Mager, T. R., "An Extensive Study of Low Fatigue Crack Growth Rates in A533 and A508 Steels," *Stress Analysis and Growth of Cracks*, American Society for Testing and Materials, ASTM STP 513, 1972, pp. 141-176.
- Hudak, S. J. Jr, Saxena, A., Bucci, R. J., and Malcolm, R. C., "Development of Standard Methods of Testing and Analyzing Fatigue Crack Growth Data," AFML-TR-78-40, May 1978.
- Forman, R. G., Kearney, V. E., and Engle, R. M., "Numerical Analysis of Crack Propagation in Cyclically Loaded Structures," *ASME Transactions, Journal of Basic Engineering*, Vol. 89, Series D, Sept. 1967, pp. 459-465.
- Walker, K., "The Effect of Stress Ratio During Crack Propagation and Fatigue for 2024-T3 and 7075-T6 Aluminum," *Effects of Environment and Complex Load History on Fatigue Life*, American Society for Testing and Materials, ASTM STP 462, 1970, pp. 1-14.
- Sullivan, A. M. and Crooker, T. W., "Analysis of Fatigue-Crack Growth in a High-Strength Steel—Part 1: Stress Level and Stress Ratio Effects at Constant Amplitude," *ASME Transactions, Journal of Pressure Vessel Technology*, Vol. 98, 1976, pp. 179-184.
- Yuen, A., Hopkins, S. W., Leverant, G. R., and Rau, C. A., "Correlations Between Fracture Surface Appearance and Fracture Mechanics Parameters for Stage II Fatigue Crack Propagation in Ti-6Al-4V," *Metallurgical Transactions*, Vol. 5, 1974, pp. 1833-1842.
- Branco, C. M., Randon, J. C., and Culver, L. E., "Influence of Mean Stress Intensity on Fatigue Crack Growth in an Aluminum Alloy," *Journal of Mechanical Engineering Science*, Vol. 17, 1975, pp. 199-205.
- Schijve, J., "Some Formulas for the Crack Opening Stress Level," *Engineering Fracture Mechanics*, Vol. 14, 1981, pp. 461-465.
- deKoning, A. U., "A Simple Crack Closure Model for Prediction of Fatigue Crack Growth Rates Under Variable-Amplitude Loading," *Fracture Mechanics: Thirteenth Conference*, Richard Roberts, Ed., American Society for Testing and Materials, ASTM STP 743, 1981, pp. 63-85.

¹⁵Colliapriest, J. E., "An Experimentalist View of the Surface Flaw Problem," *The Surface Crack: Physical Problems and Computational Solutions*, J. L. Swedlow, Ed., American Society of Mechanical Engineers, 1972, pp. 43-62.

¹⁶Speidel, M. O., "Stress Corrosion and Corrosion Fatigue Crack Growth in Aluminum Alloys," *Stress Corrosion Research*, Hans Arup and R. N. Parkins, Eds., Sijthoff and Noordhoff, Alphen aan den Rijn, The Netherlands, 1979, p. 135.

¹⁷Amateau, M. F., Hanna, W. D., and Kendall, E. G., "Fatigue Crack Growth in Ti-6Al-4V from Threshold to Unstable Fracture," Space and Missile Systems Organization, Los Angeles, CA, SAMSO TR 368, No. 30, 1973.

¹⁸Sandifer, J. P. and Bowie, G. E., "Double Exponential Functions that Describe Crack Growth Rate Behavior," AIAA Paper 77-363, March 1977.

¹⁹Annis, C. G., Wallace, R. M., and Sims, D. L., "An Interpolative Model for Elevated Temperature Fatigue Crack Propagation," AFML-TR-176, Part I, Nov. 1976.

²⁰Jaske, C. E., Feddersen, C. E., Davis, K. B., and Rice, R. C., "Analysis of Fatigue, Fatigue Crack Propagation and Fracture Data," Battelle Columbus Laboratory, NASA CR-132332, Nov. 1973.

²¹Newman, J. C. Jr., "Prediction of Fatigue Crack Growth Under Variable Amplitude and Spectrum Loading Using a Closure Model," *Design of Fatigue and Fracture Resistant Structures*, American Society for Testing and Materials, ASTM STP 761, 1982, pp. 255-277.

²²Saxena, A. and Hudak, S. J., "Evaluation of the Three-Component Model for Representing Wide-Range Fatigue Crack Growth Rate Data," *Journal of Testing and Evaluation*, Vol. 8, 1980, pp. 113-118.

²³Fitzgerald, J. H., "Empirical Formulations for the Analysis and Prediction of Trends for Steady-Static Fatigue Crack Growth

Rates," American Society for Testing and Materials, *Journal of Testing and Evaluation*, Vol. 5, 1977, pp. 343-353.

²⁴Paris, P. C., Gomez, M. P., and Anderson, W. E., "A Rational Analytic Theory of Fatigue," *The Trend in Engineering*, Vol. 13, University of Washington, Seattle, 1961, pp. 9-14.

²⁵Paris, P. C., "The Fracture Mechanics Approach to Fatigue," *Fatigue—An Interdisciplinary Approach*, Syracuse University Press, N.Y., 1964, pp. 107-132.

²⁶Swift, T., "Verification of Methods for Damage Tolerance Evaluation of Aircraft Structures to FAA Requirements," presented to the 12th International Committee on Aeronautical Fatigue, Toulouse, France, May 1983.

²⁷Elber, W., "The Significance of Fatigue Crack Closure," *Damage Tolerance in Aircraft Structures*, American Society for Testing and Materials, ASTM STP 486, 1971, pp. 230-242.

²⁸Unangst, K. D., Shih, T. T., and Wei, R. P., "Crack Closure in 2219-T851 Aluminum Alloy," *Engineering Fracture Mechanics*, Vol. 9, 1977, pp. 725-734.

²⁹Paris, P. C. and Hermann, L., "Twenty Years of Reflection on Questions Involving Fatigue Crack Growth, Pt. II: Some Observation of Crack Closure," in *Fatigue Thresholds*, Vol. I, Engineering Materials Advisory Services Ltd., United Kingdom, 1982, pp. 11-32.

³⁰Newman, J. C. Jr., "A Finite Element Analysis of Fatigue Crack Growth," in *Mechanics of Crack Growth*, American Society for Testing and Materials, ASTM STP 590, 1976, pp. 281-301.

³¹Mackey, T. L., "Fatigue Crack Propagation Rate at Low ΔK of Two Aluminum Sheet Alloys, 2024-T3 and 7057-T6," *Engineering Fracture Mechanics*, Vol. 11, 1979, pp. 753-761.

³²"Standard Test Method for Constant-Load Amplitude Fatigue Crack Growth Rates Above 10^{-8} m/cycle," E647-83, *Annual Book of ASTM Standards*, Sec. 3, Metals Test Methods and Analytical Procedures, Vol. 03.01, Metals-Mechanical Testing; Elevated and Low-Temperature Tests, American Society for Testing and Materials, 1983, pp. 710-730.

From the AIAA Progress in Astronautics and Aeronautics Series...

EXPERIMENTAL DIAGNOSTICS IN COMBUSTION OF SOLIDS—v. 63

Edited by Thomas L. Boggs, Naval Weapons Center, and Ben T. Zinn, Georgia Institute of Technology

The present volume was prepared as a sequel to Volume 53, *Experimental Diagnostics in Gas Phase Combustion Systems*, published in 1977. Its objective is similar to that of the gas phase combustion volume, namely, to assemble in one place a set of advanced expository treatments of diagnostic methods that have emerged in recent years in experimental combustion research in heterogenous systems and to analyze both the potentials and the shortcomings in ways that would suggest directions for future development. The emphasis in the first volume was on homogenous gas phase systems, usually the subject of idealized laboratory researches; the emphasis in the present volume is on heterogenous two- or more-phase systems typical of those encountered in practical combustors.

As remarked in the 1977 volume, the particular diagnostic methods selected for presentation were largely undeveloped a decade ago. However, these more powerful methods now make possible a deeper and much more detailed understanding of the complex processes in combustion than we had thought feasible at that time.

Like the previous one, this volume was planned as a means to disseminate the techniques hitherto known only to specialists to the much broader community of research scientists and development engineers in the combustion field. We believe that the articles and the selected references to the literature contained in the articles will prove useful and stimulating.

Published in 1978, 339 pp., 6 × 9 illus., including one four-color plate, \$25.00 Mem., \$45.00 List

TO ORDER WRITE: Publications Dept., AIAA, 1633 Broadway, New York, N.Y. 10019